Computations of Flow past the Corrugated Airfoil of Drosophila Melanogaster at Ultra Low Reynolds Number

B. Rohit[1], S. S. R. Reddy [2], S. Ghosh[1] and M. A. S. Shakil [3]

[1] *Rashtreeya Vidyalaya College of Engineering, India*
[2] *Indian Institute of Science, India*
[3] *Magellan Aerospace India Pvt Ltd, India*

†*Corresponding Author Email: benjaminr@rvce.edu.in*

ABSTRACT

The study of corrugated wings has become acquainted in the field of insect flight in recent times. Recent studies on the aerodynamic effects of a corrugated wing are based on insects like the Dragonfly; whereas the likes of Fruitfly (Drosophila Melanogaster) usually go unobserved due to their smaller size. Consequently, the behaviour of these corrugations is found to be anomalous especially in the low and ultra-low Reynolds number region. Therefore, the main aim of this study is to understand the aerodynamic effects of the corrugated airfoil present in the wing of a Fruitfly; by conducting a geometric parametric study during a static non-flapping flight at 1000 Re. In this computational study, a 2-D section of the corrugated wing along the chord is considered. The parametric study helps in understanding the effects of varying number of corrugations, angle of corrugations and the presence of a hump at the trailing edge. The dimensions were scaled to a suitable reference value to additionally compare the corrugated airfoil of Fruitfly to that of a Dragonfly. The present study shows that the aerodynamic performance of the corrugated wing in terms of c_l and c_d are predominantly governed by the subtle geometric variations that can largely impact the formation of bubbles, vortex zones, and their mutual interaction. The reduction in the number of leading edge corrugations improved the c_l/c_d ratio and reduction in the corrugation angle helped produce higher lift. The presence of a trailing edge hump also improved the stall angle with a better flow re-attachment. The presence of corrugation at the trailing edge proved to be more beneficial compared to the model with corrugations at the leading edge. This also helped in understanding, the aerodynamic superiority of the trailing edge corrugations present in the Dragonfly's wing when compared to the Fruitfly's.

Keywords: Bio-inspiration; Fruitfly; Dragonfly; CFD.

NOMENCLATURE

α	angle of attack		mesh node
c_l	coefficient of lift	w	specific turbulent dissipation rate (or turbulence frequency)
c_d	coefficient of drag		
k	turbulence kinetic energy	x_j	position vector
p	mean static pressure		
t	time	ρ	mean mass density
u	mean flow velocity		
Y^+	non-dimensional distance (based on local cell fluid velocity) from the wall to the first	β^*, σ^*	closure coefficients in the turbulence kinetic energy equation
		μ, μ_t	molecular, eddy viscosity

1. INTRODUCTION

Biomimicry and Bio-Inspired Engineering have become a fast-growing area of research in recent times, especially emulating insect flight and understanding the physics behind it (Sun and Tang 2002; Ellington 1991; Nachtigall 1981; Lim 2019; Bomphrey and Godoy Diana 2018; Cheng and Sun 2016; Bennett 1975; Yuan *et al.* 2008; Bennett 1966). It can be studied in two ways, one being the mechanism of flapping and the other on the geometry of the wing and the airfoil itself. A plethora of books have been published all over the last 5 decades,

which describe insect flight and aerodynamics in much detail (Pringle 2010; Goldsworthy 1989; Pringle 1975; K. 1996; Rainey 1976). An airfoil having ridges or grooves along the surface is known as a corrugated airfoil. The application of corrugated wings can also be extended to MAV (Micro Aerial Vehicle) which fly at ultra-low Reynolds number (Desért *et al.* 2017). This study mainly deals with the geometric parametric study of the corrugated airfoil of Drosophila Melanogaster (Fruitfly) and to compare the aerodynamic performance to a Dragonfly's airfoil. Far less research has been carried out on Fruitfly wings at ultra-low Reynolds number when compared to the research conducted on other insect wings such as the Dragonfly, hence the interest is to study aerodynamic behaviour of the Fruitfly's airfoil at a Reynolds number of 1000.

1.1 Literature

Research done on the corrugated wing of Dragonfly has concluded that corrugations have an aerodynamic advantage. In this section, the aerodynamic superiority of a corrugated wing structure being is demonstrated by various authors especially in the Ultra-low Reynolds number regime that is under 10^4. To obtain the geometry of the insect a micro scan of the wing was performed by Brandt *et al.* (2015). Shi *et al.* (2012) experimentally studied corrugation of the Dragonfly wing and compared it with its smoother counterpart at 2000 Reynolds number and found that during reverse flow the protruding peaks on the corrugated wing delay the flow separation thus giving aerodynamic advantage to the corrugated wing. Dragonfly wing with corrugations and trailing edge hump has also shown a better reduction in flow separation in the study conducted by New *et al.* (2014). Results found by New *et al* (2014) also indicate that a physically larger recirculating region works better than multiple small recirculating regions in mitigating flow-separation behavior. A comparison of the Dragonfly wing with a flat plate was performed numerically by (Lian *et al.* 2014) which showed that the corrugations provided better structural strength to the wing and produced higher pressure drag due to thicker virtual streamlined profile created by the stagnant vortices trapped in the valley. An experimental study on a bio-inspired corrugated airfoil was compared with a streamlined airfoil and a flat plate at Re= 58,000 - 125,000 for MAV designs by Murphy and Hu (2009). Peaks in the corrugated wing trapped the unsteady vortex which helped the boundary layer to stay attached and created a faster transition to turbulent zone when compared to a streamlined airfoil (Murphy and Hu 2009). Hu and Tamai (2008) conducted an experimental study on a bio-inspired corrugated wing to compare it with a traditional streamlined airfoil and a flat plate at the chord Reynolds number of 34,000 for MAV applications. It was reasoned that unsteady vortex between the peaks promotes the transition of the separated boundary-layer flow from laminar to turbulent which provided sufficient kinetic energy for the boundary layer to overcome the adverse pressure gradients, thus discouraging large-scale flow separations and airfoil stall (Hu and Tamai 2008). Computational study on a simplified Dragonfly wing

with a hump at the trailing edge at Re 6000 was performed by (Levy and Seifert 2010). Variation in corrugation height, rear arc and trailing edge shape was analyzed and was found that the roll-up of shear layer downstream attaches back due to the hump which leads to an increase in the lift to drag ratio (Levy and Seifert 2010). Computational work was performed at a Reynolds number of 5000 - 58000 applicable to a small unmanned aircraft on a Dragonfly wing by Barnes and Visbal (2013) with variation in leading-edge geometry. It was concluded that raising the first corrugation peak results in further stall delay and greatly enhances the lift-to-drag ratio compared to a flat plate.

The effects of corrugation on insect wings during sweeping motion at Reynolds number 200 and 3500 were studied numerically by Luo and Sun (2005). They found that corrugated wing and flat plate produced similar aerodynamic forces due to the length of the corrugation being smaller than the size of the separated flow region during sweeping motion at a higher angle of attack. Winslow *et al.* (Winslow *et al.* 2018) numerically found that the flat plate would give better lift compared to conventional airfoils at low Reynolds number as it trips the laminar boundary layer at the leading edge, allowing it to reattach further downstream. The increase in the camber on thin-plate airfoils also increased the lift to drag ratio when compared to flat plate (Winslow *et al.* 2018).

Literature suggests that corrugations give a better aerodynamic performance at ultr low Reynolds number regime (under 10^4). But few studies such as by Vargas *et al.* (2008) also suggest that flat plate works the best at low α and low Re such as 5000. As the wing of a Fruitfly has not been explored aerodynamically in much detail, the Fruitfly's airfoil geometry has been studied; giving a better understanding of the effect of corrugations.

The present study deals with various permutations of corrugations to understand the overall effects of the corrugations in an Ultra-low Reynolds number flow. Insects such as the dragon fly, tend to have the similar design but with different number of corrugations, corrugation angle and position of the corrugation and other variations such as the hump. To be able to achieve a comprehensive understanding of the formation and exact placement of the long and short bubble which are a dominant factor to determine the aerodynamic behaviour of the airfoil, various geometric permutations are studied.

The comparison of the Fruitfly and Dragonfly has been done, to distinguish the role of corrugations in the two different species.

The study and comparison flat plate is not being made in this study, due to the plethora of available research.

2. METHODOLOGY

2.1 Numerical Modelling

As the flight speed of a Fruitfly is relatively low, it

has been assumed that the flow is incompressible and laminar. Though the flow is laminar, it includes turbulent zones due to flow separation and unsteady vortices being trapped between corrugations.

The entire study was done only on a 2 D cross-section of the wing with static flight conditions. The commercial CFD software Fluent was used to predict the aerodynamic attributes of the airfoil. To study the aerodynamic effects at low Reynolds number flow near the body, the K-omega SST turbulence model was chosen. The K-omega SST model is a two-equation eddy-viscosity model as shown in Eq. (1) and Eq. (2). The K-omega SST has become quite popular in recent times due to its adaptability during adverse pressure gradients and separating flow (Menter 1994).

$$\frac{\partial(\rho k)}{\partial t} + \frac{\partial(\rho u_j k)}{\partial x_j} = P - \beta^* \rho \omega k + ...$$

$$...\frac{\partial}{\partial x_j}\left[\left(\mu + \sigma_k \mu_t\right)\frac{\partial(k)}{\partial x_j}\right] \qquad (1)$$

$$\frac{\partial(\rho\omega)}{\partial t} + \frac{\partial(\rho u_j \omega)}{\partial x_j} = \frac{\gamma}{v_t} P - \beta^* \rho \omega^2 + ...$$

$$...\frac{\partial}{\partial x_j}\left[\left(\mu + \sigma_\omega \mu_t\right)\frac{\partial(\omega)}{\partial x_j}\right]$$

$$... + 2(1 - F_1)\left[\frac{\rho_{\omega 2}}{\omega}\frac{\partial(\rho\omega)}{\partial t}\frac{\partial(\rho k)}{\partial t}\right] \qquad (2)$$

2.1.1 K-omega SST - Low-Reynolds-Number Correction

When the k - ω models are utilized at low Reynolds number as in this investigation, a low-Reynolds-number amendment to the turbulent viscosity needs to be enabled. The coefficient α^* damps the turbulent viscosity causing a low-Reynolds-number correction. The α^* rectification is given in Eq (3).

While in the high-Reynolds-number form of the k - ω model, $\alpha^* = \alpha^*_\infty = 1$.

$$\alpha^* = \alpha^*_\infty \left(\frac{\alpha^*_0 + \mathrm{Re}_t / R_k}{1 + \mathrm{Re}_t / R_k}\right) \qquad (3)$$

Where

$$\mathrm{Re}_t = \frac{\rho k}{\mu \omega}, \quad R_k = 6, \quad \alpha^*_0 = \frac{\beta_i}{3}, \quad \beta_i = 0.072$$

The simulations were first run in steady state until the solution converged. To be able to obtain a time independent result the study was performed under transient state, which also helped in capturing the temporary change in parameters. The flight Reynolds number of a Fruitfly is around 1000, hence velocity was calculated according to the chord

Reynolds number formula.

2.2 Validation of the Numerical Model

To validate the numerical model, a Dragonfly airfoil geometry was chosen from the work done by Hord (2012). The domain dimensions with a radius of 5c in the inlet and walls at a distance of 15c and the outlet at 10c; where the chord length is 100mm. The velocity was calculated to be 0.146 m/s considering a 100mm chord and boundary conditions were velocity inlet, stationary walls with the no-slip condition and pressure outlet. The turbulent intensity was kept as 1% and the transient analysis was conducted with a time step of 0.001. Boundary conditions are given in table 1.

Table 1 Boundary conditions in CFD setup

Reynolds Number	1000
Inlet Velocity	0.146m/s
Density	1.225 kg/m^3
Viscosity	1.7894 x 10^5 Ns/m^2

2.3 Meshing and Grid Sensitivity

The mesh for all models was created using tetrahedral elements. Hexahedral elements were not chosen as they are usually good for symmetric and even geometries, they can result in very high aspect ratios and skew values which can give erroneous results for complex geometries like a corrugated wing.

The model was meshed with various tetrahedral element sizes and checked for the convergence of c_l values. A grid sensitivity analysis was carried out, where it was found that as the mesh element size was decreased the c_l values started to converge as depicted graphically in Fig. 1. Below the 20mm mesh size, the results were constant, hence this element size was chosen to mesh both Dragonfly and the Fruitfly model. This also helps in saving computational time. Also to set the wall distance accurately a Y+ value analysis was carried out. The value of Y+ must be below 1 for a K-omega SST model, which was obtained when the maximum mesh element size was below 20mm across the domain as shown in Fig.1. The mesh size of 20mm sets the max size of a mesh element in the entire domain, in this case 20mm sized elements are found at the extreme walls of the domain and the mesh gets gradually denser towards the body to obtain computational efficiency.
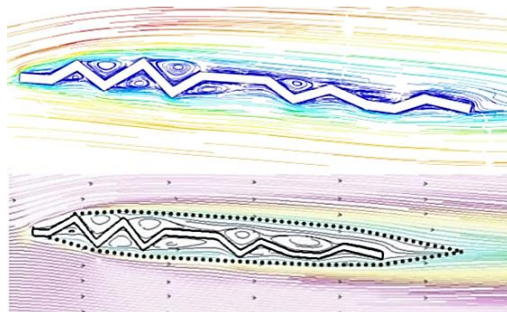
2.4 Comparison of the Dragon Fly Results

The results obtained were verified from previously published data by Hord (2012), where a Dragonfly airfoil was studied numerically at various α with varying Reynolds number of 500, 1000 and 2000.

Table 2 compares the numerical results from the present study to the results obtained by Hord (2012) in terms of c_l and c_d, the results matched within a scatter of 5.26% for all cases. Figure 2 compares the

results obtained in the present with the results obtained by Hord (2012) at 4 degree α. The flow patterns are also found to be identical at 8 and 12 degree α.
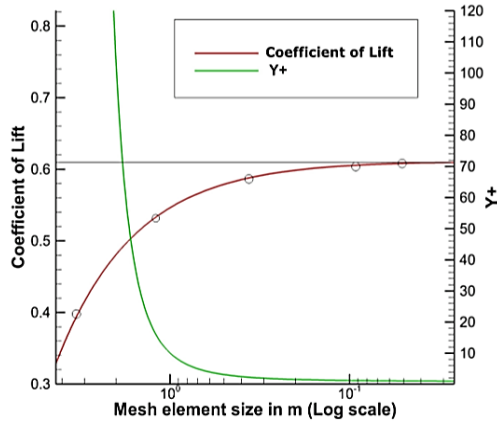
Fig. 1. Mesh convergence to validate an experimental c_l value of 0.61 at 12 degrees α at 1000 Re and a Y+ convergence is also achieved as the mesh size decreases.

Table 2 Comparison of numerical data with data from the work by Hord for a Dragonfly wing

AoA(a)	c_d – Hord(Hord 2012)			c_d numerical		
	Re-500	Re-1000	Re-2000	Re-500	Re-1000	Re-2000
0	0.19	0.11	0.09	0.18	0.11	0.09
4	0.19	0.14	0.10	0.19	0.14	0.11
8	0.20	0.16	0.12	0.21	0.16	0.13
12	0.22	0.18	0.18	0.22	0.18	0.18
16	0.31	0.32	0.35	0.31	0.32	0.35
20	0.40	0.40	0.41	0.42	0.40	0.39
AoA(a)	c_l – Hord (Hord 2012)			c_l numerical		
	Re-500	Re-1000	Re-2000	Re-500	Re-1000	Re-2000
0	0.05	0.05	0.05	0.05	0.06	0.05
4	0.31	0.35	0.30	0.31	0.35	0.31
8	0.51	0.50	0.48	0.51	0.51	0.52
12	0.61	0.62	0.63	0.60	0.61	0.65
16	0.80	0.90	1.00	0.79	0.86	0.97
20	0.92	1.20	0.99	0.89	1.18	0.94

Fig. 2. Comparison plots with the results from the works by Hord at 4 degree α.

3. PERFORMANCE COMPARISON OF CORRUGATED FRUIT FLY AIRFOIL WITH VARYING PARAMETERS

3.1 Fruit Fly Wing Geometry

The Fruitfly's corrugated airfoil dimensions were taken from Luo *et al*. (Luo and Sun 2005). The study on sectional shapes of wings showed that it is reasonable to model the corrugation by triangular waves. Here, the corrugation was modeled by triangular waves between the leading edge and a point which is 0.6 times the chord from the leading edge as shown in Fig. 3. The average values of the wavelength and the amplitudes are 0.2c and 0.03c, respectively. The thickness was 0.03c and the chord length was chosen to be 100mm as Dragonfly model was scaled to the same ratio in literature.

Fig. 3. Geometry of the Fruit Fly wing Cross Section (All dimensions are in mm).

3.2 Varying Number of Corrugations

The original Fruitfly had 3 corrugations; hence the number of corrugations was varied as 1, 2 and 4 as shown in Fig. 4 to study the effect of the number of corrugations.
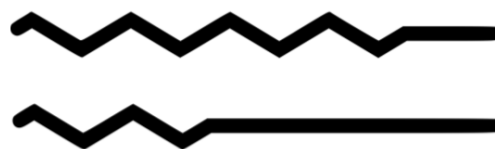
**Fig. 4. Fruitfly wing model with 2 and 4 corrugations.**

With the decrement in corrugations, the amount of lift generated increased along with increased wake drag, as an overall trend. The model with one corrugation produced the highest lift, this can be accounted to the long bubble formed at a α of 4 degrees, which creates a low-pressure zone on the suction side of the airfoil. Also, there is an initial dip in the one corrugation lift curve at 8 degrees α where the trailing edge short bubble first starts forming which interacts with the leading-edge long bubble, thus reducing the overall lift as shown in Fig. 5.
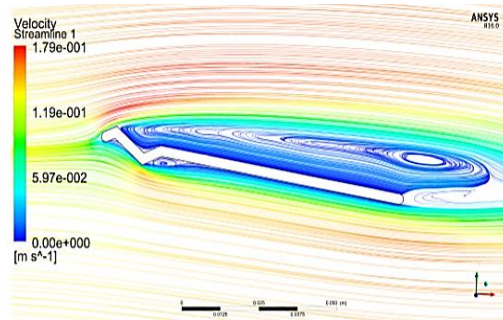
Fig. 5. Plot of streamlines for the model with a single corrugation at 8 degrees α.

As the α is increased, the two bubbles become more choate, adding to this there is a significant distance between the bubbles that avoids interference between two low-pressure zones. A similar flow phenomenon is observed in the two corrugations model, where the corrugation in the leading edge allows a vortex zone to develop as shown in Fig. 6. The flat profile further allows the long bubble to form sufficiently close to the suction surface that provides an increased lift.
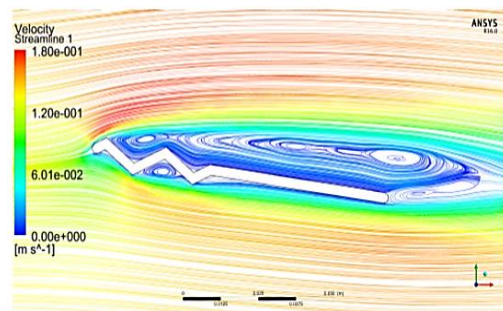
Fig. 6. Plot of streamlines for the model with two corrugation at 8 degrees α.

The flow phenomenon is different when the number of corrugations is three and four. Here the number of vortex zones formed on the upper surface is greater than the 1 and 2 corrugation models, but the effect is equally reduced due to the higher number of lower side vortex zones, hence the net increase in lift is not large. Also due to the presence of a larger number of corrugations, the long bubble that was seen in the earlier case does not form as there are breaks due to the protruding corrugations that hinder the continuity of the bubble as seen in Figs. 7. There is a linear increase in the lift with the increase in α, in the models with 3 and 4 corrugations. The interaction between the trailing edge bubble with the leading edge long bubble is not predominant near the trailing edge at the 8 degrees α mark but occurs further down-stream. As a result, the dip in the lift curve is also absent.

At α of 32 degrees and above, the c_l/c_d generated by all the models are identical because

the corrugations no longer affect the flow, and fall under a shadow region as the models approach stall.

In terms of profile drag, it is seen that the increase in corrugations does not affect the total drag of the airfoil to a large extent. The wake drag produced by the airfoils comparatively plays a more decisive role.

As discussed earlier, the formation of a trailing edge bubble starts at an α of 8 degrees which creates significant wake drag. In the lower α region (0-20 deg) the performance of the airfoils in terms of drag are alike. Whereas, when the α is increased beyond the 20 degrees mark the models behave differently. The models with a lower number of corrugations have a more choate trailing edge bubble which produces larger wake drag. In contrast, the models with a higher number of corrugations have a more gradually growing bubble that produce lesser drag. In spite of the interaction with the long bubble, the effect of the wake is not felt by these higher corrugated models due to a larger distance between the trailing edge and the interaction zone occurring further down-stream.
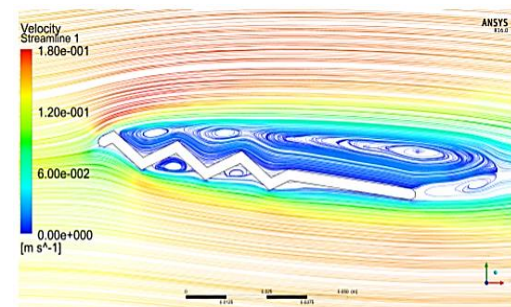
Fig. 7. Plot of streamlines for the model with three corrugation at 8 degrees α.

The c_l/c_d ratio of the models are shown in Fig. 9, lift and drag variations is shown in Fig. 8. The increase in the number of corrugations reduces the efficiency of the airfoil at a Reynolds number of 1000. The performance comparison between all the varying number of corrugations models is given in table 3.

3.3 Angle of Corrugation

The angle of corrugation on the Fruitfly's wing has also been studied. The angle on the Fruitfly's wing was found to be 118 degrees. Hence angles 100, 140 and 160 degrees were studied. The 100-degree corrugation angle is shown in Fig. 3.

In the 100-degree corrugation model, the lift produced was the least, this can be accounted to the height of the corrugation. With the increment of α, the vortex zones start to form, subsequently the long bubble forms gradually, which helps in the

Table 3 Comparison of performance when the number of corrugations increase on the Fruitfly wing

SL No	Parameter	1 Cor	2 Cor	3 Cor	4 Cor
1	Max c_l	0.934	0.91	0.9	0.858
2	Corresponding c_d	0.866	0.85	0.84	0.836
3	Max c_l/c_d	3.2	3.05	2.95	2.8
4	Stall Angle (deg)	42	42	40	44

production of lift. But the increased height does not allow the low-pressure vortex zones to fully develop in the valleys of the corrugations; the flow has an excess of kinetic energy that doesn't allow it to remain attached to the surface of these corrugations as seen in Fig. 10. Thereby, the long bubble formed is also at a greater distance from the suction surface when compared to the models with a larger angle of corrugations (shorter height). This reduces the amount of lift produced despite the formation of the long bubble.
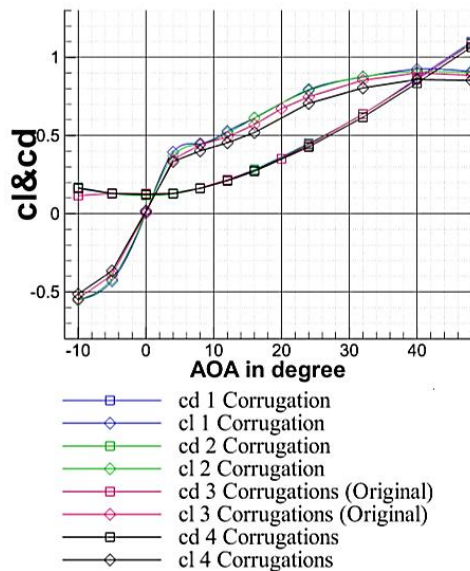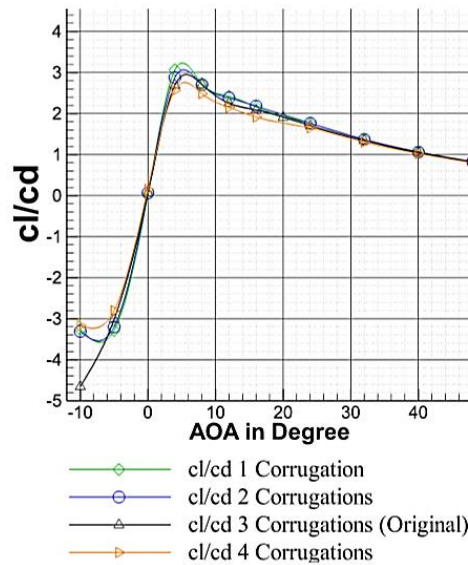

Fig. 8. Plot of c_l & c_d vs α for varying number of corrugations from 1 to 4.

In terms of lift, the 140-degree corrugation model does outperform (after 20 degrees α) the 160-degree model. This is due to the long bubble being closer to the suction surface horizontally in the 140 degrees model whereas, in the 160 degrees model, the bubble is at the trailing edge which does not contribute to the increase in lift. The bubble placement at the suction surface of the 140 degree and 160 degree model is shown in Figs. 11 and 12.

In terms of drag, the increment of angle/ decrement height of corrugations allows the long bubble not only closer to the airfoil perpendicularly but also closer to the trailing edge bubble that produces higher wake drag due to the mutual interaction between the two low-pressure zones. The effect of wake due to the short bubble in the trailing edge is the deciding factor. In the 140 degree model, the size of the short and long

bubble is bigger compared to other models. This creates higher drag as shown in Figs.13.

Fig. 9. Plot of c_l/c_d vs α for varying number of corrugations from 1 to 4.

The above observations indicate that not only is the bubble formation important for the lift but the vicinity and size of the bubble near the suction surface are equally significant. Hence, the presence of corrugations with a suitable height can allow an airfoil to produce a better lift. The c_l/c_d ratio of the models is shown in Fig. 14, overall the increase in the angle of corrugations increases the efficiency of the corrugated airfoil at a Reynolds number of 1000. The performance comparison between all the varying angles of corrugation models is given in table 4.

3.4 Presence of Hump near the Trailing Edge

A hump was added near the trailing edge of the Fruitfly airfoil model as shown in Fig. 15. The shape and geometry of the hump were inspired by the work done by Levy *et al*. (Levy and Seifert 2010). The presence of the hump helps in reattaching the flow at a higher α. Up to 6 degrees α the Fruitfly's airfoil had a better lift. This is due to the presence of a large vortex zone at the pressure side of the hump causing lesser lift as shown in Fig. 16.

After 6 degrees of α, the lift of the hump model improves and peaks up to 1.11 as shown in table 5.

Table 4 Comparison of performance when the angle of corrugations are varied on the Fruitfly wing

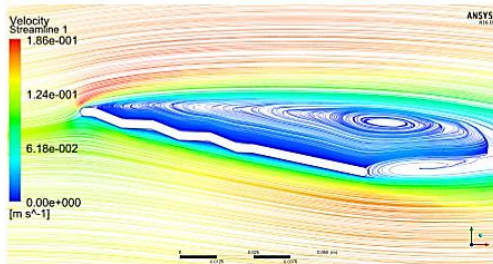| SL No	Parameter	100 deg	118 deg	140 deg	160 deg
1	Max c_l	0.867	0.9	1.16	0.94
2	Corresponding c_d	0.84	0.84	1	0.85
3	Max c_l/c_d	2.2	2.95	3.7	3.9
4	Stall Angle (deg)	48	40	42	42

The hump at the trailing edge helps in the reattachment of the flow through the formation of the bubble. As shown in Fig. 16 and in Fig. 17, due to the presence of the hump, higher no. of recirculation zones are formed on the suction side, thus increasing the overall lift. At higher α, the lift curve is nonlinear, this is due to the formation of the bubble at the trailing edge and, the interaction of this bubble with the bubble on the hump. Hence there is a sudden peak in the lift curve.
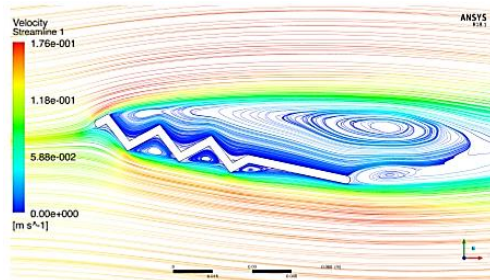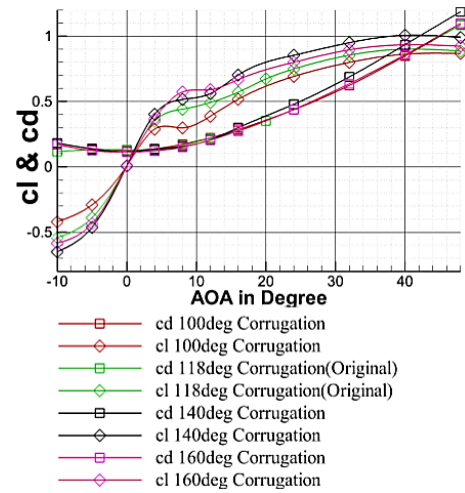

Fig. 10. Plot of streamlines for a 100 degrees corrugation model at 12 degrees α.
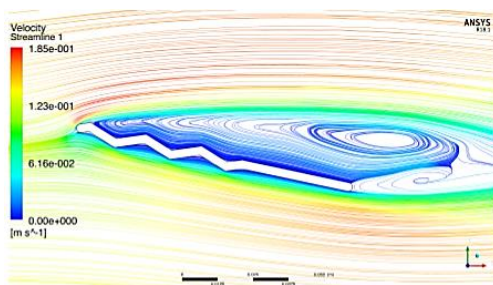
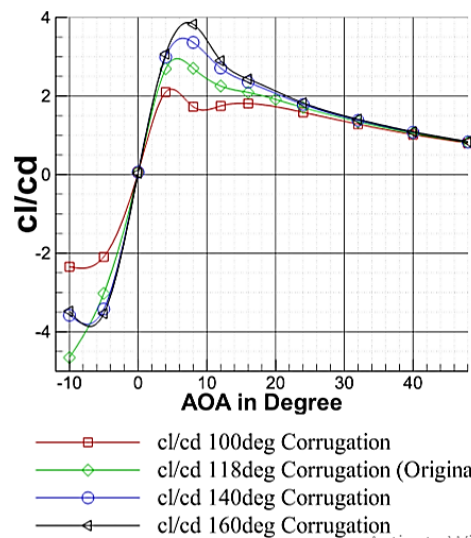**Fig. 11. Plot of streamlines for a 140 degrees corrugation model at 12 degrees α.**

Fig. 12. Plot of streamlines for a 160 degrees corrugation model at 12 degrees α.

Legend:
- cd 100deg Corrugation
- cl 100deg Corrugation
- cd 118deg Corrugation(Original)
- cl 118deg Corrugation(Original)
- cd 140deg Corrugation
- cl 140deg Corrugation
- cd 160deg Corrugation
- cl 160deg Corrugation

Fig. 13. Plot of c_l&c_d vs α for varying the angle of corrugations.

Legend:
- cl/cd 100deg Corrugation
- cl/cd 118deg Corrugation (Original)
- cl/cd 140deg Corrugation
- cl/cd 160deg Corrugation

Fig. 14. Plot of c_l /c_d vs α for varying the angle of corrugations.

In terms of drag, the hump model airfoil had a similar drag curve to that of the Fruitfly's airfoil till 20 degrees α. The hump model airfoil has a higher c_l/c_d ratio and higher stall angle due to the interaction of bubbles at the hump, which delays the flow separation as depicted in Fig. 18.
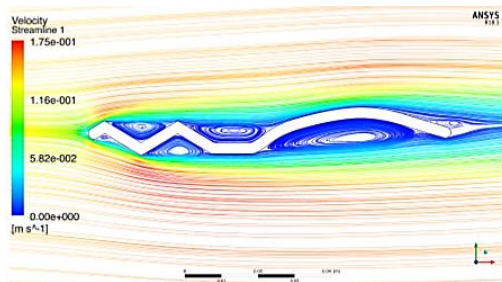
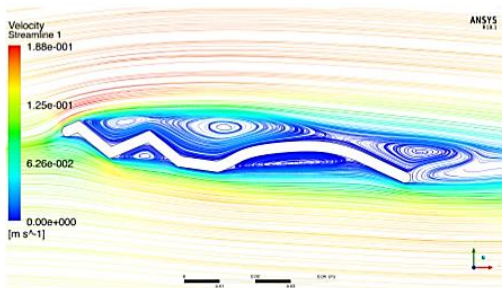**Table 5 Comparison of performance with the presence of a hump at the trailing edge of a Fruitfly wing**

SL No	Parameters	Original Model	Humped Model
1	Max c_l	0.9	1.11
2	Corresponding c_d	0.84	1.11
3	Max c_l/c_d	2.95	3.6
4	Stall Angle (deg)	40	44

Fig. 15. Fruitfly wing model with a hump.

Fig. 16. Plot of streamlines at 0 degree α to indicate higher number of recirculation zones in the hump model.
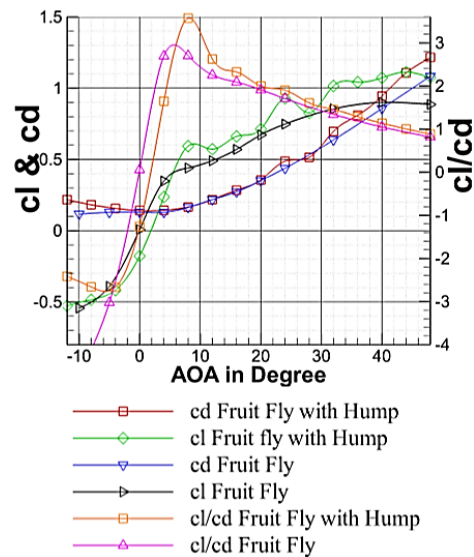

Fig. 17. Plot of streamlines at 8 degree α.

- cd Fruit Fly with Hump
- cl Fruit fly with Hump
- cd Fruit Fly
- cl Fruit Fly
- cl/cd Fruit Fly with Hump
- cl/cd Fruit Fly

Fig. 18. Plot of c_l&c_d vs α, and c_l /c_d vs α with and without hump.

Table 6 Comparison of performance of Fruitfly and Dragonfly airfoil

SL No	Parameters	Fruit Fly Model	Dragon Fly Model
1	Max c_l	0.9	1.2
2	Corresponding c_d	0.84	0.4
3	Max c_l/c_d	2.95	3.94
4	Stall Angle (deg)	40	-

3.5 Comparison of Fruitfly Airfoil with Drag- Onfly Airfoil

The Fruitfly's airfoil was compared with the Dragonfly's airfoil, whose geometry is shown in Fig. 19. Table 6 gives the performance comparison of Fruitfly and Dragonfly airfoil. From Fig. 20, it can be seen that the Dragonfly's airfoil has a better lift and c_l/c_d ratio compared to the Fruitfly. This is due to the geometry of the Dragonfly's airfoil, where the corrugations are present at the trailing edge in addition to the leading edge.

Dragonfly has a higher but similar c_l /c_d ratio trend compared to Fruitfly till 4 degrees α . But at higher α the corrugations at the trailing edge prevents flow separation due to the presence of vortex zones between the corrugations. This also contributes to higher lift generation.

3.6 Corrugations at the Trailing Edge

Based on the results from the previous section, a comparative study was performed to study the performance of corrugations at the trailing edge and the leading edge of the Fruitfly's airfoil. In terms of c_l /c_d as shown in Fig. 21, trailing edge corrugation model showed a higher c_l /c_d ratio compared to Fruitfly's leading-edge corrugation airfoil. But compared to Dragonfly, it is efficient only in the range of 0-8 degrees α . This effect is due to the presence of a higher number of vortex zones on the lower surface in the Dragonfly's airfoil which reduces the lift. The drag of the two models remains almost similar, due to the interaction of the bubbles in trailing edge corrugated model the drag is slightly higher starting from an α of 12.
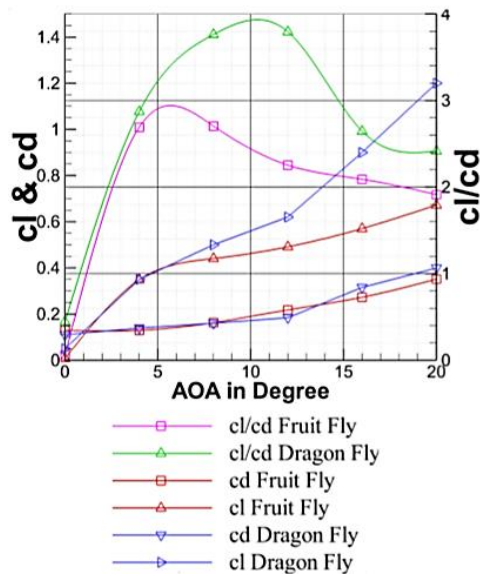
Table 7 Comparison of performance of leading edge and trailing edge corrugations

SL No	Parameters	Fruit Fly Model	Trailing Edge Corrugation Model
1	Max c_l	0.9	0.92
2	Corresponding c_d	0.84	0.87
3	Max c_l/c_d	2.95	3.96
4	Stall Angle (deg)	40	40

Fig. 19. Cross Section of the dragonfly's wing.

Fig. 20. Plot of c_l and cd vs α, and c_l /c_d vs α comparing the fruitfly's performance with a dragonfly's performance.

According to the c_l plot, the trailing edge corrugated model produces a higher lift compared to the leading edge corrugated model. Due to the placement of corrugations at the trailing edge, the size of recirculation zones on the lower side is small compared to the leading corrugations model as shown in Fig. 22. The smaller size increases the pressure on the lower side of the airfoil. It also ensures a better flow re-attachment, as the corrugations create low-pressure vortex zones on the upper surface that helps the flow to remain attached. The performance comparison is given in table 7.

At 8 degrees α, there is a peak in the lift curve of trailing edge corrugations. This can be accounted to the formation of a long bubble at the trailing edge corrugations that helps in decreasing pressure and thus increasing the lift as shown in Fig.s 22 and 23. Whereas at 4 degrees α, the long bubble is absent and only the trailing edge bubble is present. As α increases, there is an interaction of the long bubble and the trailing edge bubble which slightly decreases

the lift and increases wake drag as shown in Fig. 23.

4. CONCLUSION

Based on the detailed parametric study, the following conclusions were drawn:

1. The reduction in the number of corrugations in the leading edge of an airfoil increases efficiency in terms of c_l / c_d ratio. The reduction in the angle of corrugation is beneficial only to an extent where the long bubble can produce higher lift, in fact when it
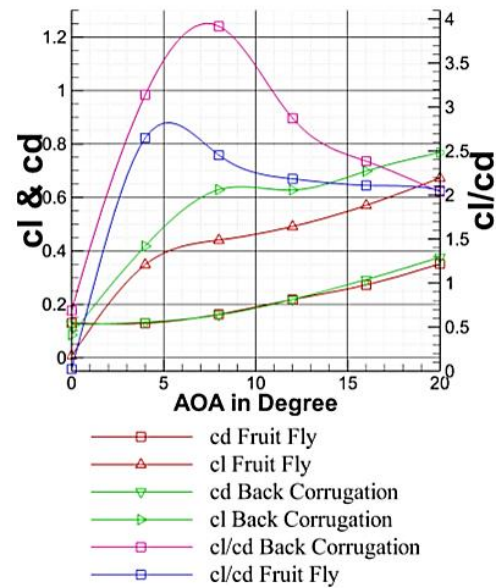
Fig. 21. Plot of c_l & c_d vs α, and c_l /c_d vs α comparing a back corrugated Fruitfly airfoil to a regular fruit fly model.
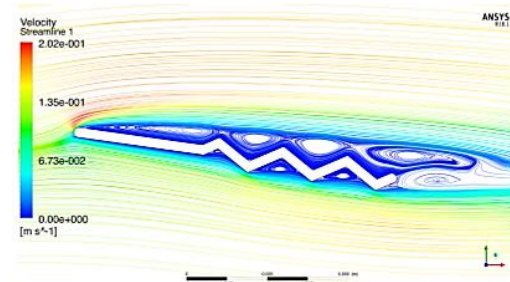
Fig. 22. Plot of streamlines at 8 degree α.
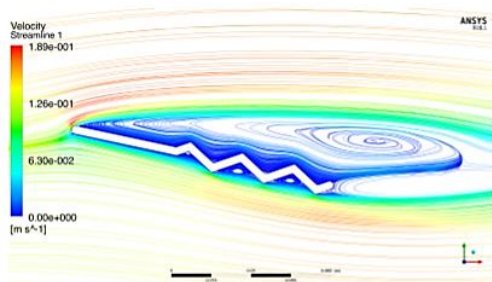
Fig. 23. Plot of streamlines at 12 degree α to visualize the presence of higher number of vortex zones.

is increased beyond a certain angle (in this case above 140) the ability to produce lift begins to drop.

2. The hump, when incorporated at the trailing edge, produced a better lift and delayed stall performance.

3. The Fruitfly airfoil was aerodynamically compared to the Dragonfly airfoil, the presence of corrugations at the trailing edge proved to be the primary difference between the two models, making the Dragonfly airfoil aerodynamically superior to the Fruitfly wing.

4. Further investigation of the effect of corrugations in the trailing edge indicated that they help in better flow re-attachment due to the formation of vortex zones. Hence it can be concluded that the corrugations in the trailing edge are more beneficial compared to the ones at the leading edge.

In terms of positioning of the bubbles seen in the study, the models with a larger long bubble, which when accommodated closer to the suction side produced the highest lift. In terms of drag, it was seen that either delay or total isolation of the long leading edge bubble and the short trailing edge bubble produced the least drag.

The outcomes of this study helped gain a better understanding of the aerodynamic behaviour of different corrugation configurations at an ultra-low Reynolds number of 1000. Using which bio-inspired airfoils can be more optimally designed for engineering applications in the field of MAV's.

REFERENCES

Barnes, C. J. and M. R. Visbal (2013). Numerical exploration of the origin of aerodynamic enhancements in [low-reynolds number] corrugated airfoils. *Physics of Fluids* 25(11).

Bennett, L. (1966). Insect aerodynamics: Vertical sustaining force in near-hovering flight. *Science* 152(3726), 1263–1266.

Bennett, L. (1975). Insect aerodynamics near hovering. *Swimming and Flying in Nature*, 815–828.

Bomphrey, R. J. and R. Godoy Diana (2018). Insect and insect-inspired aerodynamics: unsteadiness, structural mechanics and flight control. *Current Opinion in Insect Science* 30, 26–32.

Brandt, J., G. Doig and N. Tsafnat (2015). Computational aerodynamic analysis of a microct based bio-realistic fruit fly wing. *Plos One* 10(5).

Brodsky A. K. (1996). *The evolution of insect flight*. Oxford University Press.

Cheng, X. and M. Sun (2016). Wing-kinematics measurement and aerodynamics in a small insect in hovering flight. *Scientific Reports* 6(1).

Desert, T., J. M. Moschetta and H. B*é*zard (2017).´ Aerodynamic design of a martian micro air vehicle. In *7TH European Conference for Aeronautics and Aerospace Sciences (EUCASS)*.

Ellington, C. (1991). Aerodynamics and the origin of insect flight. *Advances in Insect Physiology* 23, 171–210.

Goldsworthy, G. J. (1989). *Insect flight*. CRC

Hord, K. (2012). Numerical investigation of the aerodynamic and structural characteristics of a corrugated wing. *Journal of Aircraft* 49(3).

Hu, H. and M. Tamai (2008). Bioinspired corrugated airfoil at low reynolds numbers. *Journal of Aircraft 45*(6), 2068–2077.

Levy, D. E. and A. Seifert (2010). Parameter study of simplified dragonfly airfoil geometry at reynolds number of 6000. *Journal of Theoretical Biology* 266(4), 691–702.

Lian, Y., T. Broering, K. Hord and R. Prater (2014). The characterization of tandem and corrugated wings. *Progress in Aerospace Sciences* 65, 41–69.

Lim, A. (2019). New mechanism reveals the aerodynamics of flapping insect wings. *Scilight*.

Luo, G. and M. Sun (2005). The effects of corrugation and wing planform on the aerodynamic force production of sweeping model insect wings. *Acta Mechanica Sinica* 21(6), 531–541.

Menter, F. R. (1994). Two-equation eddyviscosity turbulence models for engineering applications. *AIAA Journal* 32(8), 1598–1605.

Murphy, J. and H. Hu (2009). An experimental investigation on a bio-inspired corrugated airfoil. *47th AIAA Aerospace Sciences Meeting including The New Horizons Forum and Aerospace Exposition*.

Nachtigall, W. (1981). Insect flight aerodynamics. *Locomotion and Energetics in Arthropods*, 127–162.

New, T. H., Y. X. Chan, G. C. Koh, M. C. Hoang and S. Shi (2014). Effects of corrugated aerofoil surface features on flow-separation control. *AIAA Journal* 52(1), 206–211.

Pringle, J. W. (1975). *Insect flight*. Oxford Univ. Pr.

Pringle, J. W. S. (2010). *Insect flight*. Cambridge University Press.

Rainey, R. C. (1976). *Insect flight*. Wiley.

Shi, S. X., Y. Z. Liu and J. M. Chen (2012). An experimental study of flow around a bioinspired airfoil at reynolds number 2000. *Journal of Hydrodynamics* 24(3), 410–419.

Sun, M. and J. Tang (2002). Lift and power requirements of hovering flight in drosophila virilis. *The Journal of Experimental Biology* 205, 2413–2427.

Vargas, A., R. Mittal and H. Dong (2008). A computational study of the aerodynamic performance of a dragonfly wing section in gliding flight. *Bioinspiration & Biomimetics* 3(2).

Winslow, J., H. Otsuka, B. Govindarajan and I. Chopra (2018). Basic understanding of airfoil characteristics at low reynolds numbers (104–105). *Journal of Aircraft* 55(3), 1050–1061.

Yuan, W., M. Khalid and X. Huang (2008). Computations of flows past an insect-like flapping wing. *26th AIAA Applied Aerodynamics Conference*.